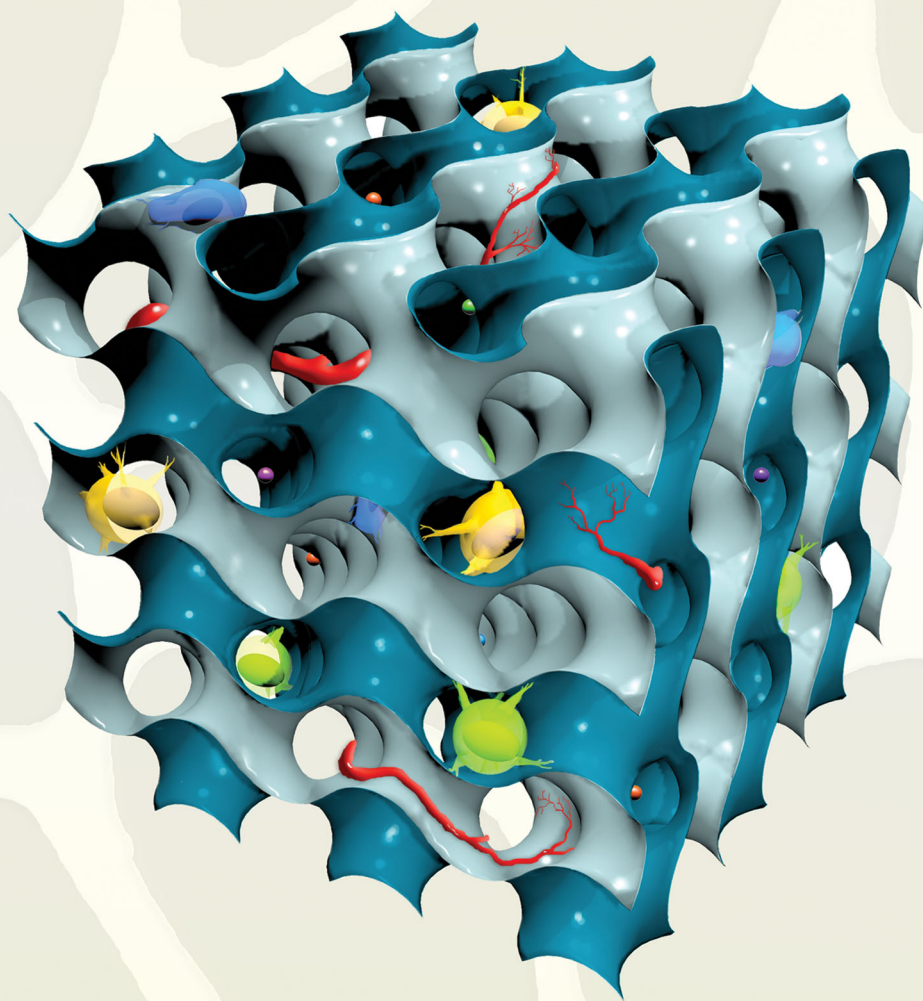


# Journal of Materials Chemistry B

Materials for biology and medicine

[rsc.li/materials-b](http://rsc.li/materials-b)



ISSN 2050-750X



## REVIEW ARTICLE

F. S. L. Bobbert and A. A. Zadpoor

Effects of bone substitute architecture and surface properties on cell response, angiogenesis, and structure of new bone



Cite this: *J. Mater. Chem. B*, 2017, 5, 6175

## Effects of bone substitute architecture and surface properties on cell response, angiogenesis, and structure of new bone

F. S. L. Bobbert\* and A. A. Zadpoor

The success of bone substitutes used to repair bone defects such as critical sized defects depends on the architecture of the porous biomaterial. The architectural parameters and surface properties affect cell seeding efficiency, cell response, angiogenesis, and eventually bone formation. The relevant parameters include pore size and porosity, pore shape and fibre orientation, surface properties, and mechanical properties. For example, small pores are preferable for cell seeding, but limit cell viability, cell proliferation and differentiation. Moreover, the pore size and geometry affect the alignment of cells and the structure of the regenerated bone. This paper presents an overview of the effects of porous biomaterial architecture including pore size and porosity, pore shape and fibre orientation, surface topography and chemistry, and structure stiffness on cell seeding efficiency, cell response, angiogenesis, and bone formation.

Received 17th March 2017,  
Accepted 2nd June 2017

DOI: 10.1039/c7tb00741h

rsc.li/materials-b

### 1. Introduction

Bone substitutes act as three-dimensional matrices that guide and promote bone regeneration in order to heal critical sized defects.<sup>1–3</sup> In these defects caused by trauma,<sup>4</sup> tumour resection,<sup>4,5</sup>

or severe fracture,<sup>5,6</sup> bone is unable to heal itself. The most common bone substitutes include autografts,<sup>7,8</sup> allografts,<sup>8</sup> and xenografts,<sup>8</sup> which are pieces of bone removed from the body of the patient, another person, or an animal, respectively.<sup>8</sup> Because the use of these biological grafts may result in damage to the body and their supply is limited, another solution has to be found.<sup>7</sup> Therefore, new synthetic biocompatible porous materials are developed. These biocompatible materials could

*Department of Biomechanical Engineering, Delft University of Technology, Mekelweg 2, Delft 2628CD, The Netherlands. E-mail: f.s.l.bobbert@tudelft.nl; Tel: +31-15-2786780*



**F. S. L. Bobbert**

*Françoise Bobbert received her BSc in Industrial Design Engineering and her MSc in Biomedical engineering at the Delft University of Technology. During her master's programme, she specialized in Tissue Biomechanics and Implants. She is currently a PhD candidate at the same university at the department of Biomechanical Engineering. The main focus of her research is the development of foldable origami structures for bone regeneration. Françoise is interested in the design of implants and tissue engineering.*



**A. A. Zadpoor**

*Amir Zadpoor is an Associate Professor and Chair of Bio-materials and Tissue Biomechanics section at the Department of Biomechanical Engineering, the Delft University of Technology. He obtained his PhD (cum laude) from the same university, and is currently interested in additive manufacturing of biomaterials, meta-materials, mechanobiology, and tissue regeneration. Amir has received several international and national awards including an ERC grant, a Veni grant, and the Early Career Award of the Journal of the Mechanical Behavior of Biomedical Materials. He has also served on the editorial boards of international journals, on the review panels of funding agencies, and as a member of award committees.*



Table 1 Biomaterial abbreviations and material group

Biomaterial abbreviation	Full form of biomaterial	Biomaterial group
CaP	Calcium phosphate	Ceramic
HA	Hydroxyapatite	Ceramic
MBG	Mesoporous bioactive glass	Ceramic
$\beta$ -TCP	$\beta$ -Tricalcium phosphate	Ceramic
Ti6Al4V	Titanium	Metal
TiNi	Titanium nickel	Metal
TT	Trabecular titanium	Metal
CSNF	Chitosan network fibres	Polymer
Col	Collagen	Polymer
CG	Collagen-glycosaminoglycan	Polymer
DEF	Diethyl fumarate	Polymer
HFIP	Hexafluoroisopropanol	Polymer
PA	Polyacrylamide	Polymer
PDMS	Poly(dimethylsiloxane)	Polymer
PLGA	Poly(lactide-co-glycolide)	Polymer
PPC	Poly(propylene carbonate)	Polymer
PPF	Poly(propylene fumarate)	Polymer
PCL	Poly( $\epsilon$ -caprolactone)	Polymer
SF	Silk fibroin	Polymer
SPCL	Starch poly( $\epsilon$ -caprolactone)	Polymer
TG	Thermoplastic gelatin	Polymer
TPU	Thermoplastic polyurethane	Polymer
PDLLA	Poly(D,L-lactic acid)	Polymer

also be called biomaterials and are not harmful or toxic to living cells and tissues inside the body.<sup>9</sup>

Depending on the biomaterial used (polymer, ceramic, or metal) (Table 1), different fabrication techniques could be applied to manufacture the designed porous biomaterials. For metal bone substitutes, selective laser melting (SLM),<sup>10–16</sup> selective laser sintering (SLS),<sup>17</sup> sintering,<sup>18</sup> perforating titanium sheet<sup>14</sup> and capsule-free hot isostatic pressing (CF-HIP)<sup>19</sup> are some examples of the applicable production methods. Polymer and ceramic bone substitutes could be manufactured with porogen leaching,<sup>20–30</sup> freeze drying,<sup>31</sup> 3D printing of successive fibre/strut layers,<sup>32–36</sup> electrospinning,<sup>37</sup> or gas foaming.<sup>1,38</sup> The above-mentioned techniques vary in accuracy and the level of control over the parameters that describe the architecture of the scaffold.

A lot of research has been undertaken to see how the architectural parameters and surface properties of a developed bone substitute influence the bone regeneration process. Parameters determining the performance of porous biomaterials for bone tissue engineering include pore size,<sup>39–43</sup> pore shape,<sup>32,41,43</sup> porosity,<sup>39,41,43,44</sup> interconnectivity,<sup>39,42,43</sup> fibre orientation,<sup>32</sup>

surface properties,<sup>2,39,45,46</sup> and mechanical properties.<sup>39,40</sup> The design of biomimetic materials affects cell behaviour and provides guidance during tissue regeneration. Therefore, the design parameters can be chosen such that the desired cell response is elicited and the formation and structure of the new bone is guided.

Bone formation occurs in several steps starting with cell seeding<sup>47</sup> or recruitment of stem cells. In the case of cell seeding, the cell seeding efficiency can be measured, which is the number or percentage of attached cells within the structure after cell suspension is seeded.<sup>47</sup> Cell viability is important in all stages of bone regeneration and depends on the availability of nutrients<sup>48</sup> and oxygen for cells within a structure, as well as on waste removal.<sup>49</sup>

Cells should be able to migrate and distribute throughout the structure to ensure a stable bone-implant fixation and bone formation within the structure. The migration of cells is a stepwise process. First, the lamellipodia and filopodia protrude at the front of the cell and adhere to the surface of the biomaterial, which is called focal adhesion.<sup>50</sup> The cell pulls itself forward by releasing the adhesions at its back side and contracting its body.<sup>51</sup> The strength of the focal adhesions influences the cell morphology<sup>52</sup> and is thought to determine cell response and gene expression.<sup>53–55</sup>

During bone regeneration, cells proliferate and differentiate into osteoblasts which deposit a collagen matrix that becomes mineralized. The first stage, *i.e.* proliferation, takes place in the first days after seeding and consists mainly of cell division.<sup>56</sup> During this stage, cells are still able to migrate.<sup>56</sup> After proliferation, cells start to differentiate into osteoprogenitor cells until the end of the second week, and the release of alkaline phosphatase (ALP) increases.<sup>57,58</sup> In two weeks after the differentiation stage, osteocalcin (OCN) and osteopontin (OPN) are produced and secreted by the cells,<sup>57,58</sup> indicating the presence of osteoblasts<sup>57,58</sup> (Table 2). When the collagen matrix is synthesized by osteoblasts,<sup>59</sup> biomineralization is initiated and mineral crystals are formed within the collagen matrix.<sup>55</sup> In parallel with the proliferation and differentiation of cells, blood vessels form from existing vessels (angiogenesis).<sup>60</sup> These vessels create a vascular network to provide oxygen and nutrients to the cells and developing tissue within the bone substitute.<sup>60</sup> This network provides stem cells needed for bone regeneration and direct the differentiation of endothelial cells and pre-osteoblasts.<sup>61,62</sup> All these steps in the bone regeneration process

Table 2 Osteogenic markers

Marker abbreviation	Full form of marker	Expressed by
ALP	Alkaline phosphatase	Osteoprogenitor
RunX-2		Osteoprogenitor, osteoblast
OPN	Osteopontin	Osteoblast
OCN	Osteocalcin	Osteoblast
OPG	Osteoprotegerin	Osteoblast, inhibits bone resorption
Calcium		Osteoblast
Col1	Collagen type 1	Organic matrix of bone, synthesized by osteoblasts
VEGF	Vascular endothelial growth factor	Growth factor blood vessels
BSP	Bone sialoprotein	Mineralized tissue



**Table 3** Effect of pore size and porosity on cell response, angiogenesis and tissue formation. Alignment: B – bridging, L – loose cells, S – sheet forming, Morphology: S – spread, E – elongated, R – round, Angiogenesis: V – VEGF, Tissue formation: B – bone, F – fibrous tissue, C – collagen. *In vitro* results and *[in vivo]* results. \* after 2 weeks of culture. No significant difference between groups cultured without OM (osteogenic medium)

Pore size and porosity		Seeding cells/ implantation site	Pore size [ $\mu\text{m}$ ] (porosity [%])	Seeding efficiency	Cell viability	Migration	Alignment	Morphology	Proliferation	Osteogenic differentiation	Angiogenesis	Tissue formation	Mineralization	Ref.
Biomaterial	Porosity [%]													
SF	hMSC		112–224 (94) 400–500 (96) 112–500 (95)	+										23
PCL	L929		84 116 141 162	++ ++ + +	– – + +		R							71
PLGA	3T3 fibroblasts		94 (36) 123 (45) 147 (58)	++ + –	++ + ++		S S/L S	S S S+	– + ++					1
SF	BMSC		80–150 (71) 150–200 (80) 200–250 (87) 250–300 (94)	– + + –	– + + +				– + + +	– + + +				72
SF	hASC		140 (76) 254 (87)	+ +	+ +				+ +	+ +		B+ B+	+ +	22
Decellularized bovine bone	hESC		208 (70) 315 (80) 376 (88)	++ + –	+ + +				– + +	+ + +		B B+ B	+ + ++	44
CG	MC3T3		85 120 325	– + ++	– – +				– + ++					31
PLGA	MC3T3		100–300 100–400 100–500	– + ++	– + ++			R S S	– + ++				– + ++	20
Ti6Al4V	hPDC		500 1000	+ –	– +				– +	– +				12
PCL + OM	hBMSC		38, 312 325	+ –	++ +				++ +	++* +			+ ++	38
PDLLA	MG63		<275 (87) <325 (88) <420 (85)	– + +	– + +		L L/S S	R S S	– + ++	– + +		C– C+ C+	– + +	24
PCL	ASC		355–500 (65) 500–1000 (65) 1000–1500 (65)	+ + +	+ + +		B B/S S	R/E R/E S	+ ++ ++	+ ++ ++			– + ++	73



Table 3 (continued)

Pore size and porosity		Seeding cells/ implantation site	Pore size [ $\mu\text{m}$ ] (porosity [%])	Seeding efficiency	Cell viability	Migration	Alignment	Morphology	Proliferation	Osteogenic differentiation	Angiogenesis	Tissue formation	Mineralization	Ref.	
Biomaterial	Seeding cells/ implantation site														
PLGA-CaP	rBMSC/rat calvarial defect	470–590 (85)	+	+	+	+	+	+	[+]	[B+]	26				
		590–850 (85)	+	+	+	+	+	+	[–]	[B]					
		850–1200 (85)	+	+	+	+	+	+	+	[–]	[B]				
PPF/DEF	BMSC	> 500							V+				21		
		180–300							V						
B-TCP	/Rabbit fascia lumbodorsalis	337 (73)												27	
		415 (74)													
		557 (71)													
		631 (72)													
PLGA	/Rat proximal tibia	100–300 (86)												81	
		300–500 (87)													
		500–710 (87)													
Ti6Al4V	/Rat femoral defect	490 (88)												11	
		490 (68)													

and the architecture of the bone substitute determine the amount and quality of the newly formed bone.

Understanding the effects of the architecture of a bone substitute on cell response is important to optimize the design of porous biomaterials that are aimed for bone regeneration. This paper presents an overview of the effects of various architectural parameters and surface properties on the cell seeding efficiency, cell response, angiogenesis, and bone formation.

The seeded cell types were mainly BMSCs, (pre-) osteoblasts, and fibroblasts. Only in a limited number of cases the cell behaviour seemed to depend on the type of seeded cells.<sup>63–65</sup>

## 2. Pore size and porosity

Pores are the voids within a porous biomaterial which provide space where new tissue and blood vessels will grow.<sup>66,67</sup> The pore size (diameter of an individual void) and porosity (percentage of void volume within a porous biomaterial) are connected to each other when the bone substitute contains an interconnected pore network. An increase in pore size has been associated with an increased porosity in most studies. Increasing the porosity of a porous bone substitute is a way to lower the stiffness.<sup>68</sup> This reduces the mismatch between the stiffness of a (metal) bone substitute and the host bone,<sup>69</sup> thereby mitigating the problems associated with stress shielding.<sup>70</sup>

### 2.1 Cell seeding efficiency

The seeding efficiency (Table 3) depends on the number of attachment sites within a porous biomaterial and the available time for cells to attach to the surface.<sup>12</sup> With an increased pore size, the surface area within the structure decreases, resulting in less attachment sites for the seeded cells.<sup>20,31</sup> In addition to the lower number of attachment sites caused by bigger pores and higher porosity, the permeability of the porous biomaterial increases.<sup>12</sup> A higher permeability value is associated with a higher flow rate, which reduces the time for cell attachment to the surface of the structure during seeding.<sup>12</sup>

Several studies have shown that the seeding efficiency decreases as the pore size increases, regardless of the biomaterial or seeding cells used.<sup>1,12,38,44,71</sup> Cells are more likely to aggregate at the seeding surface of poly( $\epsilon$ -caprolactone) (PCL) porous biomaterials with pores smaller than 84  $\mu\text{m}$ .<sup>71</sup> This results in an inhomogeneous distribution of cells throughout the structure.<sup>71</sup> In structures with bigger pores (*e.g.* 116  $\mu\text{m}$ ), cells are able to penetrate the top surface and distribute homogeneously throughout the scaffold.<sup>71</sup> However, when pores become larger (> 162  $\mu\text{m}$ ), cells tend to escape from the structure.<sup>71</sup> In a study by Salerno *et al.*, PCL structures seeded with hMSCs with a bi-modal architecture (mean pore sizes 38  $\mu\text{m}$  and 312  $\mu\text{m}$ ) and a mono-modal structure (mean pore size 325  $\mu\text{m}$ ) were compared.<sup>38</sup> They found that cells distributed throughout the bi-modal scaffolds, but that they remained in the seeding region of the mono-modal scaffolds.<sup>38</sup> Studies with silk fibroin (SF) scaffolds found a low seeding efficiency with no difference among scaffolds with pore sizes between 80 and 500  $\mu\text{m}$ .<sup>22,23,72</sup>



One explanation for this low seeding efficiency of these scaffolds is their high porosity which ranged between 71% and 96%. In general, small pores are preferable for cell seeding. However, these pores should be larger than 100  $\mu\text{m}$  to make a homogeneous distribution throughout the porous biomaterial possible. Depending on the tortuosity of the void space, there is a limit to the pore size to prevent cell escape which will reduce the seeding efficiency.

## 2.2 Cell viability

Cell viability seems to be mainly affected by the pore size and the porosity of the biomaterial (Table 3). Different studies<sup>1,12,20,31,44,72</sup> found a higher cell viability in porous biomaterials with bigger pores, which can be related to the higher oxygen diffusion into the interior region of these structures.<sup>20</sup> The oxygen diffusion within porous biomaterials with small pores is limited by cell aggregation at the surface and the low penetration level during cell seeding and migration. In decellularized bone scaffolds, no difference in cell viability was found for different pore sizes and porosities.<sup>44</sup> The difference in these findings might be the result of the structure thickness, the pore size and porosity of these porous biomaterials, and the tortuosity of the void network. The porosity (and pore size) of different porous biomaterials varied between 71% and 94% (80–300  $\mu\text{m}$ ) (SF),<sup>72</sup> 36–58% (94–147  $\mu\text{m}$ ) poly(lactide-co-glycolide) (PLGA),<sup>1</sup> 42–87% (500–1000  $\mu\text{m}$ ) (Ti6Al4V)<sup>12</sup> and for the decellularized bone substitutes between 70.4 and 88.3% (208–376  $\mu\text{m}$ ).<sup>44</sup> The lower cell viability in the SF<sup>72</sup> and PLGA (Fig. 2c)<sup>1</sup> scaffolds with small pores can be explained by the pore size which was smaller than 100  $\mu\text{m}$ . In these scaffolds, cells are more likely to aggregate and block the way for oxygen and nutrients to the centre of the scaffolds. Based on these results, it could be concluded that pores smaller than 100  $\mu\text{m}$  should be avoided to prevent cell death.

## 2.3 Cell migration

Cell migration depends on the pore size and porosity of a porous biomaterial (Table 3).<sup>1,20,24,31,38,44,71,72</sup> Restricted cell migration was observed in porous biomaterials with small pores, while cells can migrate more easily and distribute homogeneously when a structure contains bigger pores up to 500  $\mu\text{m}$ .<sup>20,31,44</sup>

## 2.4 Cell alignment and morphology

Table 3 summarizes the results found on cell alignment and morphology (Fig. 1). In large pores, cells tend to align with and

form sheets on the pore walls<sup>1,24,44,73</sup> while cells are able to bridge smaller pores.<sup>69,73</sup> The sheet formation occurred in PCL scaffolds with pores between 1000 and 1500  $\mu\text{m}$ .<sup>73</sup>

In a study on Ti structures with a mean pore size of 425  $\mu\text{m}$ , cells elongated and connected with other cells and the pore walls in pores whose size was between 100 and 150  $\mu\text{m}$ .<sup>69</sup> Pores larger than 200  $\mu\text{m}$  could not be bridged and the cells aligned with the pore surfaces.<sup>69</sup> No cell growth was found in pores smaller than 100  $\mu\text{m}$ .<sup>69</sup>

The sheet-formation of cells could be connected to a well-spread cell morphology<sup>10,19,25,33,72,74</sup> (Fig. 1c–f) with filopodia adhered to different points on the pore surface, indicating strong focal adhesions.<sup>69,75</sup> These filopodia help the cell sheets to align within the pores.<sup>75</sup> Cells that bridge small pores or several struts are subjected to higher strains than cells adhered to a single surface, depending on the ratio between the cell size and pore size or the distance between the struts.<sup>76</sup> Cell sheets are formed by filopodia of cells that are connected to neighbouring cells, leading to a better communication between cells.<sup>77,78</sup> Furthermore, a close connection with the pore surface seems to improve the bone regeneration process.<sup>73</sup> By modifying the pore size, the alignment within the pores and the cell morphology could be guided. However, the pore shape and biomaterial used should be taken into account as well.

## 2.5 Cell proliferation

Cell proliferation depends on the amount of nutrients to produce a new cell and the available space for cells to grow and multiply.<sup>69,79</sup> The pore size and porosity are important to satisfy these requirements, resulting in higher proliferation rates in porous biomaterials with bigger pores and higher porosities<sup>1,12,20,24,31,44,69,72,73</sup> (Table 3). Porous biomaterials with large pores have more space for cell growth and enhance the diffusion of oxygen and nutrients. In the bi-modal and mono-modal PCL scaffolds mentioned before, the hMSCs within the seeding region of the mono-modal scaffolds proliferated faster than the cells within the bi-modal scaffolds up to 21 days after seeding.<sup>38</sup> This was due to the higher availability of oxygen and nutrients at the top of the scaffolds compared to the centre and the bottom of the scaffold.<sup>38</sup> However, due to the high number of cells within the top part of these mono-modal scaffolds after three weeks, lack of space led to a reduction of living cells.<sup>38</sup> A higher cell number was found within decellularized bone,<sup>44</sup> SF,<sup>72</sup> PLGA<sup>20</sup> and collagen-glycosaminoglycan (CG)

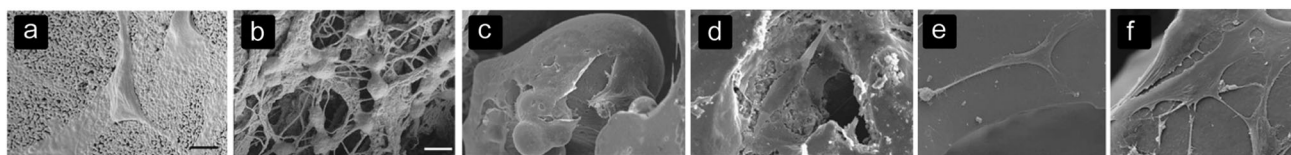


**Fig. 1** Cell alignment and morphology on different biomaterials with different surfaces and architectures. (a) Spreading of BMSCs on the surface of HA structures,<sup>85</sup> (b) BMSCs bridging several collagen fibers within the HA structure,<sup>85</sup> (c) spreading of osteoblasts and forming sheets on a convex surface in NiTi structures,<sup>19</sup> (d) osteoblasts adjusting the morphology to the roughness of pores in NiTi structures,<sup>19</sup> (e) stretched morphology of BMSCs on the MBG surface after 7 days,<sup>74</sup> and (f) BMSCs show a well-spread morphology and connecting to other MBSs after 7 days on MBG structures with a silk film created with a 5.0% silk solution.<sup>74</sup>



scaffolds containing more pores with a minimum size of 200–300  $\mu\text{m}$ .<sup>31</sup> Studies on PLGA-CaP<sup>26</sup> and SF<sup>22</sup> structures with pores between 140 and 1200  $\mu\text{m}$  did not find a significant difference in cell proliferation. It is difficult to determine why some studies found a significant difference in proliferation and some did not. The materials (PLGA and SF) were used in the studies that found a significant difference in proliferation for larger pores as well as in studies that did not. Also, the pore sizes used in the latter studies were in the range of the pore sizes used in the studies in which pore size seemed to affect cell proliferation. And finally, the seeding cells used (ASCs and BMSCs) also do not seem to be the reason for the different findings. Therefore, it is not clear what pore size would promote cell proliferation.

## 2.6 Cell differentiation

The results in Table 3 imply that the pore size may affect cell differentiation. Studies on porous SF<sup>22</sup> and decellularized bone<sup>44</sup> structures found no significant difference in alkaline phosphatase (ALP) expression between structures with different pore sizes. However, an initially higher ALP activity was found in SF scaffolds (Fig. 2h) with bigger pores.<sup>72</sup> This might suggest that small pores delay osteogenic differentiation. Studies on poly(propylene fumarate) (PPF),<sup>21</sup> PLGA-CaP,<sup>26</sup> PCL,<sup>74</sup> poly(D,L-lactic acid) (PDLLA),<sup>24</sup> Ti6Al4V<sup>12</sup> and SF<sup>72</sup> scaffolds found an increased osteogenic differentiation in scaffolds with larger pores.

In a study on bi-modal and mono-modal PCL scaffolds, higher OPN levels were found at the top of scaffolds with a mono-modal architecture.<sup>38</sup> In those scaffolds, the seeded cells remained at the top of the scaffold and therefore faster proliferation and osteogenic differentiation occurred due to the high availability of oxygen and nutrients and exposure of cells to osteogenic medium.<sup>38</sup> One explanation that osteogenic differentiation occurred more in large pores is that the cells tend to be more spread in large pores compared to small pores. This morphology is thought to promote osteogenic differentiation.<sup>53</sup>

## 2.7 Blood vessel formation

Angiogenesis occurs by the formation of small branches at the ends of existing blood vessels<sup>80</sup> that grow into the bone substitute.<sup>19</sup> The production of vascular endothelial growth factor (VEGF) is needed to stimulate the growth of these small blood vessels<sup>80</sup> and is found to be higher in porous PPF biomaterials (Fig. 2e) cultured *in vitro* with large pores (Table 3).<sup>21</sup> When insufficient blood vessels are present during the bone regeneration process, fibrous tissue will form.<sup>80</sup> Fibrous tissue was found in porous biomaterials with small pores in an *in vivo* study on  $\beta$ -tricalcium phosphate ( $\beta$ -TCP) scaffolds.<sup>27</sup> In the same study, more blood vessels with a bigger diameter were present and less fibrous tissue was formed in substitutes with pores bigger than 400  $\mu\text{m}$ .<sup>27</sup> It was also observed that porous biomaterials with pores between 470 and 590  $\mu\text{m}$  contained more blood vessels as compared

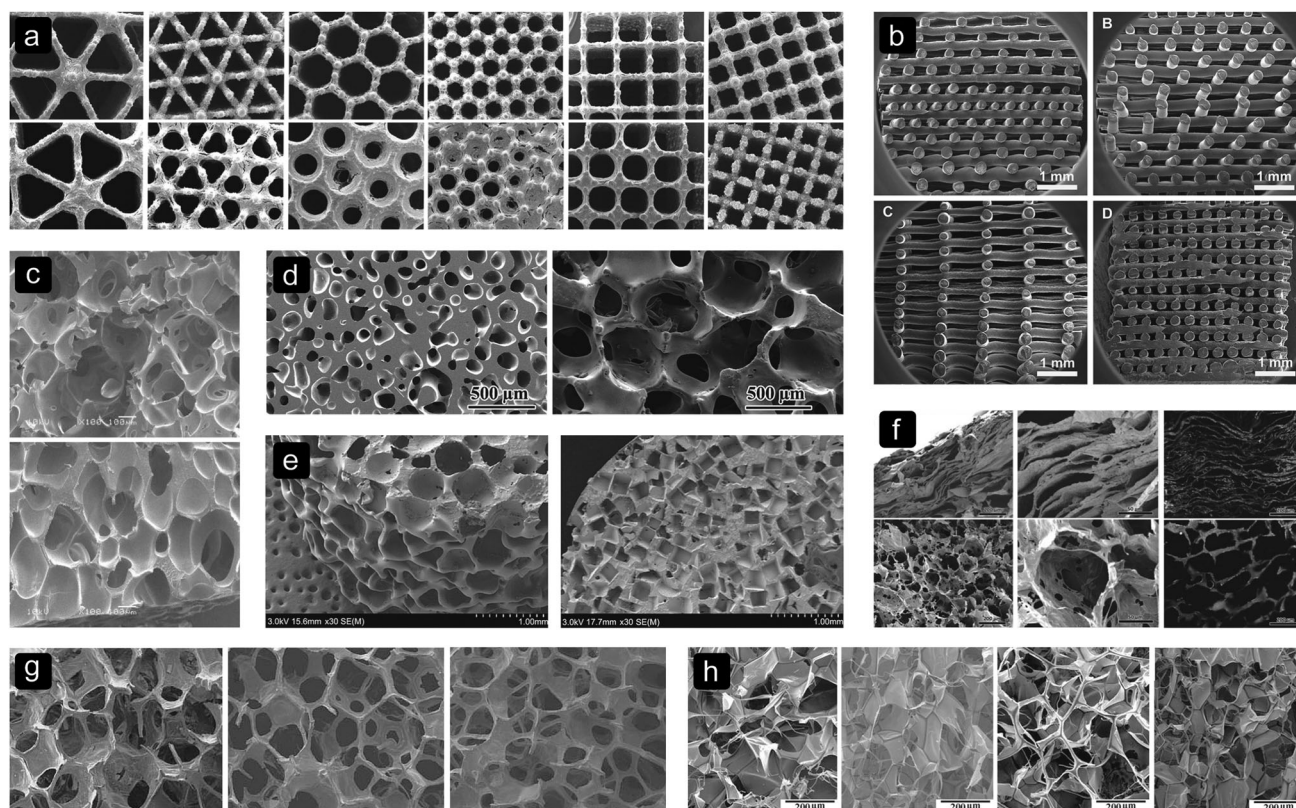


Fig. 2 Different pore sizes, shapes and biomaterials. (a) Ti6Al4V,<sup>12</sup> (b) SPCL,<sup>103</sup> (c) PLGA,<sup>1</sup> (d) BG,<sup>87</sup> (e) PPF,<sup>21</sup> (f) collagen-apatite,<sup>64</sup> (g) MBG,<sup>74</sup> and (h) SF.<sup>72</sup>



to porous biomaterials with pores larger than 590  $\mu\text{m}$ .<sup>26</sup> These results seem to suggest that pores larger than 400  $\mu\text{m}$  are preferable for blood vessel formation and consequently for the delivery of oxygen and nutrients to the cells inside the bone substitute.

### 2.8 Tissue formation and mineralization

Tissue formation and mineralization in porous biomaterials are affected by pore sizes and porosities (Table 3). In the initial stage, *i.e.* up to 2 weeks of *in vitro* culture, collagen structures were unorganized in a PDLLA structure.<sup>24</sup> After this period, they became more complex and structurally organized.<sup>24</sup> This was also found in implanted PLGA structures with a higher amount of collagen in structures with large pores compared to structures with small pores.<sup>81</sup> Thicker collagen fibres were present in PDLLA scaffolds with medium sized pores compared to scaffolds with larger and smaller pores.<sup>24</sup> Also the amount of mineralized collagen was higher in scaffolds with medium sized pores compared to the scaffolds with large pores, and no calcium areas were found in scaffolds with the smallest pores ( $< 275 \mu\text{m}$ ).<sup>24</sup>

Porous biomaterials with larger pores were found to have a better and higher distribution of calcium and mineral deposition parallel to the pore walls *in vitro*.<sup>73</sup> This could be an effect of the alignment of cells with the pore walls, higher cell viability, distribution, and proliferation rate in structures with large pores.

An *in vitro* study showed increased bone formation in scaffolds with medium sized pores, which could be related to the higher amount of osteoblasts present in the inner region of these scaffolds.<sup>44</sup> Different *in vivo* studies have shown that a higher porosity promotes host bone ingrowth for a stable fixation with the bone substitute<sup>11,70</sup> and that larger pores suppress fibrous tissue infiltration.<sup>27</sup> In an *in vivo* study by Sicchieri *et al.*, most bone was formed in scaffolds with pores between 470 and 590  $\mu\text{m}$ .<sup>26</sup> The limited amount of fibrous tissue infiltration and high amount of bone formation in large pores seem to be related to the higher amount of space and blood vessels present in these structures. Therefore, it can be concluded that large pores and angiogenesis are important for bone formation.

### 2.9 Structure of the new bone

The structure of the new bone grown *in vivo* depends on the organization of the synthesized collagen, which seems to be affected by the pore size<sup>81</sup> (Table 3). It was observed that cells tend to align with the walls of big pores where they proliferate, differentiate, and synthesize a structured collagen matrix. When this matrix becomes mineralized, it forms a lamellar structure.<sup>81</sup> Therefore, the alignment of cells with the pore walls in bigger pores could be used to control the structure of the newly formed bone. In a study on PLGA scaffolds with different pore size ranges of 100–300, 300–500 and 500–710  $\mu\text{m}$ , the most newly formed bone with a lamellar structure was found in scaffolds with the medium pore size range.<sup>81</sup>

## 3. Pore shape and fibre orientation

The geometry of pores within a bone substitute can be, among others, spherical, rectangular, square, hexagonal or trabecular-like, depending on the biomaterial and manufacturing process used (Fig. 2). With solid freeform fabrication techniques, even more complex shapes can be realized (Fig. 3).<sup>82,83</sup> The pore size and shape affect the mechanical properties of porous biomaterials, as they determine the dimensions and orientation of the struts or fibres and, thus, the stress distribution inside those structural elements.<sup>12,13</sup> Moreover, stress concentrations due to the notches present inside the structure or caused by manufacturing imperfections could affect the mechanical behaviour of porous biomaterials.<sup>13</sup>

Scaffolds with a ladder-like structure and rectangular pores and scaffolds with large spherical pores collapse more easily than porous biomaterials with smaller uniform round pores.<sup>25</sup> Studies on the mechanical properties of Ti6Al4V structures (Fig. 2a) with different pore shapes (diamond, cube, truncated cuboctahedron, triangular, and hexagonal) showed different mechanical properties<sup>12</sup> and fatigue strength for different unit cells with similar porosity.<sup>13</sup>

### 3.1 Seeding efficiency

In the studies evaluated (Table 4), not much research has been done on the seeding efficiency of different pore geometries. A study on SF scaffolds found no difference in the seeding efficiency of lamellar structures or structures with spherical pores.<sup>22</sup> However, in a study where PCL scaffolds consisted of random or oriented fibres, a higher seeding efficiency was found in the scaffolds with a random fibre orientation.<sup>34</sup> This random architecture created a more tortuous void space and therefore a better geometry for cells to attach to during seeding.

### 3.2 Cell migration

The effects of pore shape and fibre orientation on cell migration can be found in Table 4. Cell migration is limited in collagen-apatite (Col-apatite) structures with lamellar pores compared to spherical pores.<sup>64</sup>

In the lamellar structure, the pores are channels with a height of 30  $\mu\text{m}$ , divided by Col-apatite layers (Fig. 2f). The cellular structure has a more honeycomb-like structure with large interconnected pores of 242  $\mu\text{m}$  (Fig. 2f). The limited cell migration in the lamellar structure may have been caused by the lower interconnectivity and small distance between the lamellae as compared to spherical pores.

Cell migration behaviour changes for different pore shapes. On a concave poly(dimethylsiloxane) (PDMS) surface with a depth of 100  $\mu\text{m}$  and a diameter of 200  $\mu\text{m}$  the cells tried to escape, while the cells on convex surfaces with similar dimensions moved on top of the convex shape.<sup>84</sup> A slow migration on flat surfaces was observed.<sup>84</sup>

### 3.3 Cell alignment and morphology

The pore shape influences the cell alignment and the rate and level of pore size reduction by cells within a porous





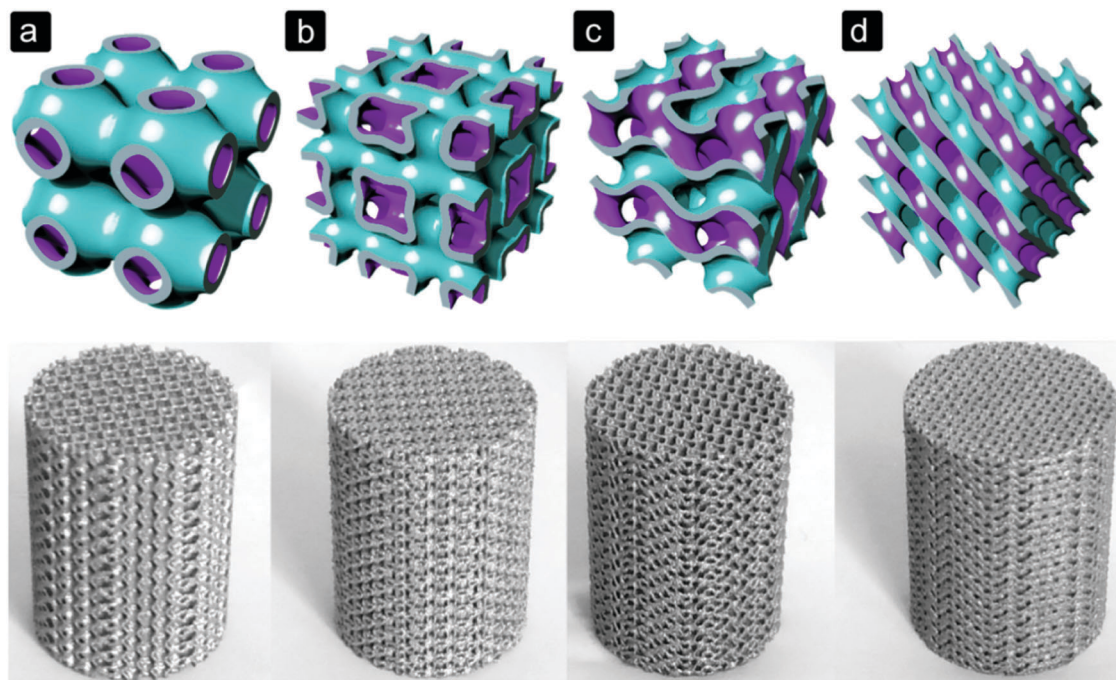


Fig. 3 Selective laser melted Ti6Al4V porous biomaterials for bone regeneration based on triply periodic minimal surfaces.<sup>104</sup> (a) primitive, (b) I-WP, (c) gyroid, and (d) diamond.

biomaterial<sup>10,12,22,25</sup> (Table 4). *In vitro* studies have shown that cells tend to bridge small distances between struts or fibres, making the pores circular-shaped.<sup>10,12</sup> Circular pores and pores with wide angled corners, like honeycomb pores, are reduced in size more and faster by cells that elongate and span short distances than pores with sharp corners.<sup>12</sup> Cells on hydroxyapatite (HA) scaffolds including a collagen fibre network connected with several collagen fibres, while the cells on the pure HA scaffolds with round pores were well spread on the pore surface<sup>85</sup> (Fig. 1a and b). These results suggest that porous biomaterials with sharp cornered pores and an open space can delay pore size reduction by cells and consequently improve the transport of nutrients, oxygen, and waste removal. An *in vitro* study on cell behaviour on convex and concave PDMS micro-patterns found that the cells on convex and flat surfaces had a well spread morphology.<sup>84</sup> A more round morphology of the cells was found on concave micro-patterns.<sup>84</sup>

### 3.4 Cell proliferation

The effect of pore shape and fibre orientation is summarized in Table 4. On PCL scaffolds with randomly oriented fibres, *in vitro* cell proliferation was found to be higher compared to orthogonal oriented fibres.<sup>34</sup> This random organization with a more tortuous architecture also improved the seeding efficiency and therefore, more cells throughout the scaffold were able to proliferate.<sup>34</sup> Triangular pores in Ti6Al4V scaffolds also showed a higher amount of cell proliferation compared to hexagonal and rectangular pores. This may be due to the amount of cells that bridged the small distances compared to the other two geometries. Therefore, there was more space in the triangular pores for cells to proliferate.<sup>12</sup> This higher amount of space also

seemed to be the reason why SF structures with spherical pores performed better in terms of cell proliferation compared to the lamellar structures.<sup>22</sup>

### 3.5 Cell differentiation

Cell differentiation seems to be affected by the pore size and fibre orientation (Table 4). In an *in vitro* study by Van Bael *et al.* (Fig. 2a), triangular pores with a size of 500  $\mu\text{m}$  could induce osteogenic differentiation while hexagonal pores and rectangular pores could not.<sup>12</sup> Another *in vitro* study found that osteogenic differentiation is affected by the orientation of a fibre network.<sup>34</sup> A higher ALP activity was found in random fibre structures compared to PCL structures with an organized orientation of fibres.<sup>34</sup> The higher amount of cells in these scaffolds due to the higher seeding efficiency,<sup>34</sup> lower reduction of pore size<sup>12</sup> and higher proliferation<sup>12,34</sup> may be the reason why more osteogenic differentiation took place.

### 3.6 Blood vessel formation

Angiogenesis seems to be affected by the organization of fibres within a porous biomaterial<sup>85</sup> (Table 4). An *in vivo* study by Scaglione *et al.* found many blood vessels in the void space of HA and HA/Col scaffolds after two months of implantation.<sup>85</sup> In HA/Col scaffolds, where there was no controlled orientation of the collagen fibres, large blood vessels grew randomly towards the centre of the structure.<sup>85</sup> In pure HA scaffolds, where more blood vessels were found, they grew through the interconnected pore network into the scaffold.<sup>85</sup> HA scaffolds with concave pores have been found to be more suitable for angiogenesis in the early stages of implantation, while convex pores promote blood vessel formation after 3 months of implantation.<sup>62</sup>





**Table 4** Effect of pore shape and fibre orientation on cell response, angiogenesis and tissue formation. Alignment: B – bridging, S – sheet forming, Morphology: S – spread, E – elongated, R – rounded. Tissue formation: B – bone, LB – lamellar bone, RB – random bone, CB – cortical bone, C – callus. *In vitro* results and *in vivo* results. ^ more host bone integration in scaffolds seeded with BMSC compared to OPCs. \* exceeded amount of calcium and blood vessels after 3 months of implantation

Pore shape and fibre orientation		Seeding cells/ implantation site	Pore shape [µm] (porosity %)	Seeding efficiency	Cell viability	Migration	Alignment	Morphology	Proliferation	Osteogenic differentiation	Angiogenesis	Tissue formation	Mineralization	Ref.
Biomaterial	hASC													
SF		hASC	Spherical 140 (76) Spherical 254 (87) Lamellar 126 (64)	+	+	+			+	+	+	+	+	22
PCL		BMSC	Fibre orientation • Oriented • Oriented offset • Random	– – +	+	+		S S S	+	+	+	–	+	34
Ti6Al4V		hPDC	Triangular 500 Hexagonal 500 Rectangular 500	+	+	+		B B+ B	++ + +	++ + +				12
PPC + chitosan fibre network (CSFN)		BMSC/rabbit femoral condyle	– CSFN 300–350 (92) + CSFN 300–350 (92) Fibre 50–500 nm	+	+	+		S S + B	+	+		[B]	+	86
Col-apatite		BMSC, OPC/mouse calvarial defect	Spherical 242 (95) Lamellar 30 (95)	+	–	–		E E		[+] [+]		[LB^] [CB+^]	[+] [+]	64
PDMS		L929 hMSC	Flat Concave Convex	+	++	–		S S O	+	– +				84
HA-Col		BMSC/mouse ectopic model	HA (80) HA + collagen fibres 250–450 (80)					S B		[+] [+]		[LB]		85
HA		/Canine dorsal muscle	Concave Convex							[–] [+*]		[C] [LB]	[–] [+*]	62
HA		/Rabbit radial diaphysis	Bi-layer outside 200, Inside 450 (68) Trabecular 440 (66)							[+]		[B]		88
13–93 BG		/Rat calvarial defect	Oriented 50–150 (50) Trabecular 100–500 (80)							[+]		[B+]		87

### 3.7 Tissue formation and mineralization

Results of various studies imply that the inner geometry of porous biomaterials affects the structural organization of the synthesized collagen (Table 4). In an *in vivo* study, HA scaffolds incorporated with a random orientation of collagen fibres within the pores showed an unorganized deposition of collagen 1.<sup>85</sup> The pure HA scaffolds with a round pore shape contained a more organized network of collagen fibres which was deposited parallel to the pore wall.<sup>85</sup> In an *in vivo* study on scaffolds with concave and convex pores, more calcium and collagen were deposited in scaffolds with concave pores.<sup>62</sup> However, after three months of implantation, the scaffolds with convex pores contained more collagen and calcium.<sup>62</sup> The fibre orientation<sup>86</sup> and pore shape<sup>62,64,87</sup> seemed to influence *in vivo* bone formation and apatite crystal deposition within the collagen matrix.

*In vitro*<sup>22</sup> and *in vivo*<sup>87,88</sup> bone formation seems to be enhanced in porous biomaterials with a trabecular architecture.<sup>22,87,88</sup> Different studies found better bone ingrowth and integration with host bone in trabecular scaffolds compared to oriented bioactive glass (BG)<sup>87</sup> (Fig. 2d) and SF<sup>22</sup> scaffolds. After 24 weeks, more bone was grown in from the sides and bottom of the scaffolds and small bone areas were present within the trabecular BG implants.<sup>87</sup> This indicates that osteoblasts were present within the scaffold and were able to form apatite crystals. In scaffolds with lamellar pores, more bone was formed after 4 weeks of implantation as compared to cellular shaped pores.<sup>64</sup> The addition of a chitosan fibre network to PPC scaffolds led to more *in vivo* bone formation compared to pure PPC scaffolds.<sup>86</sup> The higher amount of cells within these scaffolds due to the higher cell viability and higher proliferation may be the reason why more bone formed in these scaffolds compared to the pure PPC scaffolds.

### 3.8 Structure of the new bone

The pore shape seems to affect the structure of the new bone (Table 4). This was found in an *in vivo* study by Yu *et al.*, where a lamellar or cellular structure (Fig. 2f) seeded with either OPCs or BMSCs was placed inside a bone defect.<sup>64</sup> In the lamellar structure, cortical like bone was formed, while a bone structure similar to trabecular bone was formed within the cellular structure (Fig. 4).<sup>64</sup> They also found that BMSCs promoted host bone integration with the scaffolds, while OPCs did not.<sup>64</sup>

The *in vivo* formed bone in pure HA scaffolds with an ordered inner geometry had a lamellar structure with collagen fibres deposited parallel to the pore wall, while the orientation of collagen fibres and bone formation on the HA/Col scaffolds was random.<sup>85</sup> Active osteoblasts were still present in HA/Col scaffolds after two months, which indicates that woven bone was present in these scaffolds.<sup>85</sup> Thin lining cells that control the mineral composition of bone were covering the new bone formed in the HA scaffolds.<sup>85</sup> Structures with convex pores induced *in vivo* formation of lamellar bone with osteoblasts and osteoclasts, while almost no mature bone was found in structures with concave pores.<sup>62</sup> This might be related to the higher vascularity in the structures with convex pores.<sup>62</sup>

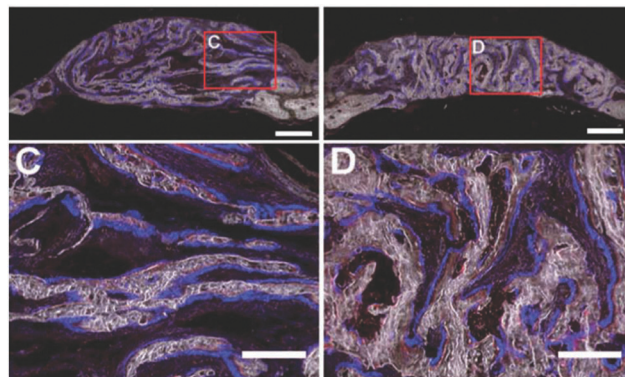


Fig. 4 Formation of new bone in collagen-apatite scaffolds after 4 weeks.<sup>64</sup> C – cortical bone structure formed in structures with lamellar structures loaded with OPCs. D – trabecular bone structure formed in structures with a lamellar architecture loaded with OPCs.

## 4. Surface topography and chemistry

Surface characteristics are important for adhesion, attachment, and spreading of cells on the surface of biomaterials.<sup>89</sup> In addition to the biomaterial a bone substitute is made of, the use of surface treatments,<sup>16</sup> addition of a silk<sup>74</sup> or CaP coating,<sup>17</sup> and integration of HA particles,<sup>25,28,29,37</sup> or HA whiskers,<sup>30</sup> may affect the surface roughness and can improve the bioactivity of a porous biomaterial.<sup>58</sup> Incorporation of CaP coatings, such as HA particles or whiskers, are thought to improve bone formation in porous biomaterials.<sup>58</sup> It is thought that due to the similarity between the composition of CaPs and bioapatite, cells would respond in a similar way as during natural bone remodelling.<sup>58</sup>

### 4.1 Seeding efficiency

A higher surface roughness is associated with a higher surface area<sup>90</sup> to which cells can attach during seeding. Various studies have shown (Table 5) that the initial attachment and seeding efficiency increases with an increased surface roughness in Ti6Al4V<sup>16,91</sup> and HA<sup>92</sup> structures, or surface chemistry of PCL/nHA porous biomaterials.<sup>28</sup> In contrast to these findings, silk scaffolds with an increased HA micro-particle content showed a lower seeding efficiency despite a higher surface roughness.<sup>29</sup> In a study on mesoporous bioactive glass (MBG) scaffolds (Fig. 2g) incorporated with a silk film within the pores to reduce the surface roughness, no significant difference in seeding efficiency was found.<sup>74</sup> Although a higher surface roughness increases the surface area and would therefore be preferable for improved seeding efficiency, contradictory results were found. It seems that a significant difference in surface roughness may indeed increase the seeding efficiency. However, the seeding efficiency does not seem to be affected when there is no significant difference in surface roughness between the compared samples.

### 4.2 Cell attachment and morphology

Cells adapt their morphology according to the surface topography of porous biomaterials<sup>2,28,35,74,92</sup> (Table 5). A higher



**Table 5** Effect of surface roughness and chemistry on cell response, angiogenesis and tissue formation. Alignment: B-bridging, S-sheet forming, Morphology: S – spread, E – elongated, R – rounded. Tissue formation: B – bone, LB – lamellar bone, WB – woven bone. *In vitro* results and *in vivo* results

Surface roughness and chemistry		Seeding cells/ implantation site	Surface roughness [ $\mu\text{m}$ ]	Seeding efficiency	Cell viability	Migration	Alignment	Morphology	Proliferation	Osteogenic differentiation	Angiogenesis	Tissue formation	Mineralization	Ref.
Ti6Al4V	hPDC/rat femoral defect	Untreated		+			B/S		+			B	+	16
		Alkali-acid (100–200 nm)		+			B/S		+			B+	++	
		Alkali-acid-heat (100–200 nm)		++			B/S		++			B	+	
		Anodizing-heat (nanotubes)		+			B/S		+++			B	++	
Silk	hBMSC	0% HA (smooth)		++					–			B	+	29
		1.6% HA (rough)		+					+			B+	+	
		3.1% HA (rough+)		+					+			B++	+	
		4.6% HA (rough +)		–					+			B++	+	
Ti6Al4V	hBMSC	0.320		+			B	E/S	++	+				91
		0.490		+			B	E/S	+					
		0.874		++			B	E/S	+					
HA	hBMSC	0.733		+			B	E/S	++	+				92
		2.856		+			B	E/S	+	+				
		4.680		++			B	E/S	+	+				
MBG	BMSC	MBG (rough)		+			S	E/S	–	+				74
		MBG + 2.5% silk (smooth)		+			S+	E/S	+	+				
		MBG + 5.0% silk (smooth)		+			S+	E/S	+	++				
PLGA	MC3T3	PLGA (smooth)		+				S	+	+				37
		+5% HA (rough)		+				S+	+	++				
TPU (HA particles)	3T3	TPU		+			S	S						25
		TPU + <i>m</i> HA		+			S	S						
		TPU + <i>n</i> HA		+			S	S					+	
Collagen	mASC	Collagen					B	E	+	–				30
		40% HA whiskers		+			B	E	–	+				
		80% HA whiskers		+			B	E	–	+				
PCL	MG-63	PCL				L	R	+					28	
		PCL + <i>n</i> HA				S	S	++						
PCL	hBMSC	0.21					S	+	+	–				35
		1.06					R	+	+	+			+	
CaP/gelatin	hOPC/rabbit radial diaphysis	Unpatterned					E	–		–				2
		50 $\mu\text{m}$ grooves					S	–		–				
		40 $\mu\text{m}$ pits					S	+		+				
Ti grade 2 (+nanoscale modification (NM))	MG63	0.43					++	++	++	++				93
		0.37 + NM					+	+	+	+				
		3.29					+	+	+	+				
		2.80 + NM					+	+	+	+				

Table 5 (continued)

Surface roughness and chemistry		Seeding cells/ implantation site	Surface roughness [ $\mu\text{m}$ ]	Seeding Cell efficiency viability	Migration	Alignment	Morphology	Proliferation	Osteogenic differentiation	Angiogenesis	Tissue formation	Mineralization	Ref.
Biomaterial	Seeding cells/ implantation site												
HA	/Pig latissimus dorsi	Non-microporous fibres Microporous fibres 2–8 $\mu\text{m}$		+	+						[–] [LB, WB]		36
Titanium 200–400 $\mu\text{m}$ pores	/Canine femoral defect	Untreated (smooth) Anodized (nanotubes) Heat-treated + anodized (nanotubes)									[B] [B]	– –	18
											[B+]	+	

surface roughness of PCL/nHA<sup>28</sup> and calcium phosphate (CaP)<sup>2</sup> scaffolds elicited a more spread cell morphology, while a higher surface roughness of PCL<sup>35</sup> and MBG<sup>74</sup> scaffolds drove hBMSCs to a less spread and more rounded morphology (Fig. 1e and f). On HA,<sup>92</sup> Ti6Al4V,<sup>91</sup> thermoplastic polyurethane (TPU),<sup>25</sup> and collagen<sup>30</sup> structures no difference in cell morphology was found. The cells were spread on the surface of all scaffolds. These contradictory results may imply that not only surface roughness but also surface chemistry affect the cell morphology. The surface properties of a biomaterial determine how well the cells can attach to the surface, which in turn affects their morphology.

### 4.3 Cell proliferation

The results in Table 5 suggest that adding HA to porous biomaterials may improve cell proliferation.<sup>28,29,92</sup> A higher cell proliferation rate was found on HA scaffolds with a smooth surface<sup>92</sup> and in scaffolds with nHA whiskers.<sup>28,29</sup> On titanium structures, the number of cells increased upon increasing the surface roughness.<sup>91,93</sup> Cell attachment and proliferation were significantly different between Ti6Al4V porous biomaterials with an arithmetical mean roughness ( $R_a$ ) of 0.32  $\mu\text{m}$  and 0.87  $\mu\text{m}$ .<sup>91</sup> Given this difference, it seems that hBMSCs are sensitive to a surface roughness difference of about 0.6  $\mu\text{m}$ .<sup>91</sup> A study by Kumar *et al.* showed an equally good proliferation rate on etched and unetched PCL scaffolds with  $R_a$  values of 1.1 and 0.2  $\mu\text{m}$ , respectively.<sup>35</sup> Although the variation in  $R_a$  was more than 0.6  $\mu\text{m}$  and hBMSCs were used, the different outcome may have been caused by different surface chemistry or stiffness of these porous biomaterials.

### 4.4 Cell differentiation

While the higher surface roughness of PCL scaffolds created by etching had no effect on the cell proliferation and caused a more rounded morphology of the cells (Fig. 1), more osteogenic differentiation of hBMSCs occurred<sup>35</sup> (Table 5). A higher surface roughness seems to improve cell differentiation on Col-HA<sup>30</sup> and MBG<sup>74</sup> scaffolds while smooth surfaces tend to slow down osteogenic differentiation. In contrast to these results, more osteogenic differentiation was present in Ti structures with a lower surface roughness.<sup>93</sup> In two other studies on HA<sup>92</sup> and Ti6Al4V,<sup>91</sup> where the surface roughness was significantly different between the tested samples, no difference in osteogenic differentiation was found. Although cell morphology is thought to affect the type into which cells differentiate, these contradictory results do not seem to show this relationship.

### 4.5 Tissue formation and mineralization

Fixation of a porous biomaterial with bone is facilitated by friction, mechanical interlocking, and chemical bonding.<sup>94</sup> The highest bond strength, mineralization, and bone formation were found in Ti6Al4V porous biomaterials with anatase nanotubes compared to structures with non-bioactive nanotubes and structures without treatment after three months of *in vivo* implantation<sup>18</sup> (Table 5). A higher bond strength can be related to a higher surface roughness, which promotes osseointegration.<sup>2,95</sup>



*In vivo* implanted HA scaffolds with increased surface roughness upon the addition of microporous rods contained newly formed bone in the centre, top, and periphery of the scaffolds, while bone was only present at the periphery of HA scaffolds without porous rods.<sup>36</sup> This could be explained by the presence of rhBMP-2 and blood vessels in the centre of the scaffolds which supplied mesenchymal stem cells.<sup>36</sup> Due to the microporous rods, more rhBMP-2 and HA surface area was present in these scaffolds compared to HA scaffolds without rods, bone formation was more promoted in these scaffolds.<sup>36</sup> A higher amount of *in vitro*<sup>25,29,37</sup> bone formation<sup>29,30</sup> and mineralization<sup>25,29,37</sup> in scaffolds with HA particles<sup>25,29,37</sup> seems to imply that the addition of HA improves osteogenesis. Applying surface treatments to bone substitutes can also change the surface chemistry and roughness to improve mineralization. It was shown that different surface treatments of Ti6Al4V structures change these properties.<sup>16</sup> *In vivo* apatite formation and osseointegration were the highest in structures treated with an acid-alkali (AcAl), while anodized-heat (AnH) treated and as-manufactured (AsM) structures showed the lowest apatite formation.<sup>16</sup> Although the AnH treated specimens did not stimulate apatite formation, they had the best mechanical stability when tested under torsion.<sup>16</sup> This may be due to their higher surface roughness with micropits and nanotubes on their surface, which improved mechanical interlocking and the mechanotransduction pathways of the cells on the surface.<sup>16</sup>

## 5. Structure stiffness

Biomaterials that are used for bone substitutes could be roughly divided into three groups, *i.e.* metals, ceramics, and polymers,<sup>96</sup> with different mechanical properties. The stiffness of metals is in general higher than the elastic modulus of bone, while the stiffness of polymers is lower<sup>97</sup> (Table 6). Consequently, the load transfer varies and leads to different stress and deformation patterns throughout the implant.<sup>94</sup>

During migration, cells adhere to the surface of the porous biomaterial and pull themselves forward.<sup>51</sup> Through their adhesions to the surface, cells apply forces to the structure and sense the stiffness of this structure.<sup>89,98</sup> Although it is assumed that cell attachment depends on the structure stiffness,<sup>55,89</sup> no effect of the stiffness on the migration of cells was found in the studies evaluated.

### 5.1 Seeding efficiency

Not many studies investigated the effect of structural stiffness on the seeding efficiency (Table 6). One study on the stiffness of PDMS scaffolds found a higher seeding efficiency on the softest structures, which decreased with increasing stiffness.<sup>63</sup> However, on PPF scaffolds (Fig. 2e), a similar seeding efficiency was found on structures with different stiffnesses.<sup>21</sup> Despite the lack of studies on seeding efficiency and substrate stiffness, there does not seem to be a connection between these two.

### 5.2 Cell viability

The structure stiffness does not seem to affect the cell viability (Table 6) of polyacrylamide (PA) scaffolds with a stiffness in the

range of 0.5–26 kPa.<sup>65,99</sup> However, a study on thermoplastic gelatin (TG)-gel scaffolds found a lower cell viability on scaffolds with a lower structure stiffness.<sup>100</sup> Due to the limited and contradictory results, no conclusion can be drawn on the relationship between the substrate stiffness and cell viability.

### 5.3 Cell alignment and morphology

It was assumed that the structure stiffness would affect the cell morphology, where a well-spread morphology would induce osteogenic differentiation.<sup>53</sup> Although differences in morphology were found on TG-gel<sup>100</sup> and PA<sup>101</sup> scaffolds with different stiffnesses, cells on substrates with a higher stiffness were not necessarily more spread (Table 6). A study on PA scaffolds showed that cells were more rounded on substrates with a stiffness of 10 and 23 kPa compared to substrates with a stiffness of 34 kPa.<sup>101</sup> However, the cells were more spread on the scaffolds with a stiffness of 34 kPa compared to the scaffolds with a stiffness of 40 kPa.<sup>101</sup> In another study, cells were more rounded on TG-gel structures with a higher stiffness compared to the softest scaffold.<sup>100</sup> Although the morphology of cells was different on structures with different stiffnesses, a higher stiffness did not necessarily lead to a more spread cell morphology.

### 5.4 Cell differentiation

A higher stiffness of hexafluoroisopropanol (HFIP)<sup>46</sup> and MBG<sup>74</sup> scaffolds achieved by the addition of silk microfibers, improved early hMSC differentiation into the osteogenic lineage (Table 6). This was also observed in PPF scaffolds with a higher stiffness due to the incorporation of diethyl fumarate (DEF).<sup>21</sup> In PDMS<sup>63</sup> and PA<sup>65,99</sup> scaffolds, the stiffest scaffolds also showed the most osteogenic differentiation. On the PDMS structures, either BMCs or AMSCs were seeded to see the response of both cell types.<sup>63</sup> This study showed that BMSCs differentiated more into osteoblasts than AMSCs.<sup>63</sup> In contrast to the highest cell differentiation on the above mentioned porous biomaterials, the most osteogenic cell differentiation took place on the PA scaffolds with the second highest stiffness.<sup>101</sup> Although there did not seem to be a relationship between cell morphology and substrate stiffness, a higher stiffness resulted in general in more cells that differentiated into osteoblasts. However, as can be seen in the PA scaffolds,<sup>101</sup> there are some exceptions.

### 5.5 Tissue formation and mineralization

The implant stiffness affects integration with the host bone when there is a clear difference in stiffness (Table 6). An increased stiffness of MBG scaffolds promoted the *in vitro* formation of apatite particles,<sup>74</sup> which may be due to the highest amount of osteogenic differentiation in these scaffolds.

In an *in vivo* study on titanium implants with two completely different designs, a stable bone-implant interface was present.<sup>14</sup> However, more bone was present within and around flex-age scaffolds as compared to the stiffer selective laser melted porous biomaterials.<sup>14</sup> This suggests that structure stiffness values close to the bone also promote bone ingrowth and bone-porous biomaterial integration.





**Table 6** Effect of structure stiffness on cell response, angiogenesis and tissue formation. Morphology: S – spread, E – elongated, R – rounded. Angiogenesis: V – VEGF, Tissue formation: B – bone. *In vitro* results and *in vivo* results. \* BMSC showed higher osteogenic differentiation than AMSC. ^ Osteogenic differentiation was lower for bone-derived cells (BDCs) compared to BMSCs. Also, no significant difference in osteogenic differentiation of BDCs was found among the different scaffolds with a different stiffness

Structure stiffness		Seeding cells/ implantation site	Structure stiffness	Seeding efficiency	Cell viability	Migration	Alignment	Morphology	Proliferation	Osteogenic differentiation	Angiogenesis	Tissue formation	Mineralization	Ref.
PPF + DEF%	Rat BMSC	0% 18 MPa								–	V			21
		+10% 31 MPa		+						+	V			
		+25% 43 MPa		+						+	V			
		+33% 28 MPa		+					++	V+				
PDMS	rAMSC rBMSC	Softest		+++						–				63
		Soft		++						–				
		Middle		+						+–				
		Stiff		+–						+				
		Stiffest		–						++*				
PA	MSC	0.51 kPa		+						+			–	99
		3.7 kPa		+					++	+			–	
		22 kPa		+					+++	++			+	
PA	BMSC BDC	1.46 kPa		+						+^			+	65
		26.12 kPa		+					++^	++^			++	
TG-Gel	C2C12	1.58 kPa		–						–	[+]		–	100
		13.51 kPa		+						+	[+]		+	
		32.32 kPa		+						–	[+]		++	
PCL	MG-63	PCL 124 kPa												28
		PCL + nHA					L	R						
		275 kPa					S	S						
PA	hBMSC	10 kPa								–				101
		23 kPa								–				
		34 kPa								++				
		40 kPa								+				
MBG + silk%	BMSC	MBG 60 kPa								+			–	74
		+2.5% 120 kPa								+			+	
		+5.0% 250 kPa								++			++	
HFIP-silk + silk fibre	hMSC/mouse lateral subcutaneous pockets	Control 85.06 kPa								–				46
		+fibre S 4.52 MPa								+				
		+fibre M 9.79 MPa								++				
		+fibre L 10.64 MPa								+				
Ti6Al4V	/Sheep metatarsal bone	Flex cage 5.9 GPa											[+]	14
		Porous cylinder 8.22 GPa											[+]	

## 6. Discussion and conclusion

This paper presents an overview of how cells respond to the architecture and surface properties of porous biomaterials for bone regeneration. We have seen that the biomaterial(s) chosen for the bone substitute is responsible for the mechanical properties and surface properties and determines the applicable manufacturing process. The manufacturing technique in turn determines the accuracy and control over the architecture of the bone substitute.

For metal bone substitutes, selective laser melting (SLM),<sup>10–16</sup> selective laser sintering (SLS),<sup>17</sup> sintering,<sup>18</sup> perforating titanium sheet<sup>14</sup> and capsule-free hot isostatic pressing (CF-HIP)<sup>19</sup> were used. Those manufacturing techniques differ in terms of their production accuracy. Both SLM and SLS can be used to create complex structures<sup>10–13</sup> with a completely controlled architecture,<sup>102</sup> while porous biomaterials manufactured with CF-HIP<sup>19</sup> and sintering<sup>18</sup> had a relatively simple geometry. The size and the shape of pores between the metal powder particles can be partly controlled and acted as the void space for tissue regeneration.<sup>18,19</sup> Sheet perforation was used to cut rhombic holes into a titanium sheet which was shaped into a star.<sup>14</sup> Although the shape and size of the holes and the geometry of the sheet can be modified, no 'inner' architecture was present in these biomaterials.<sup>14</sup> The polymer and ceramic bone substitutes evaluated in this study were manufactured with porogen leaching,<sup>20–30</sup> freeze drying,<sup>31</sup> 3D printing of successive fibre/strut layers,<sup>32–36</sup> electrospinning,<sup>37</sup> or gas foaming.<sup>1,38</sup> 3D printing of fibre layers and electrospinning were used to generate fibre-based constructs with a controlled and uncontrolled architecture, respectively. It was seen that with the other techniques, the pore size, interconnectivity and pore shape could partly be controlled (Fig. 2). 3D printing is the most promising manufacturing technique for load bearing (biodegradable) metal bone substitutes because high control over the architecture of the structures can be realized (Fig. 3).

Different studies have shown that the seeding efficiency is mainly affected by the pore size of the porous biomaterials. However, more than just the pore size should be taken into account when optimizing the seeding efficiency of a structure for bone regeneration. Although it is important to prevent cells from aggregating at the seeding surface by making the pores not too small, it is also important to take the tortuosity and interconnectivity of the void space into account. Different results would be acquired when cells are seeded onto a scaffold with pores in which the cells can vertically fall through the structure or when they can only reach the bottom of the implant via tortuous pathways. Therefore, based on the tortuosity and the interconnectivity of the void space that are created with the manufacturing technique, a suitable pore size (>100 µm) should be chosen. For good progress of all the steps following cell seeding, the pores should have a minimum size of 200–300 µm.

Cell aggregation should be prevented because this can obstruct the path to the centre of the structure. Cells tend to bridge small distances which occur in small pores, in pores with sharp angles and in structures with randomly deposited fibres. It was found that it takes more time for cells to reduce

the size of the pores with wide angles or spherical pores as compared to pores with sharp angles.<sup>12</sup> This makes sense because more space is available at the corners of pores with sharp angles (triangular pores) as compared to the spherical pores with a similar pore size. If pores are large enough, cells align with the pore walls and form sheets, which leaves the void space open for oxygen and nutrients to reach the inner regions of the porous biomaterial. Because oxygen and nutrients are vital for cells to survive and proliferate, porous biomaterials with large pores are preferable for bone regeneration.

The alignment of cells with the walls of large pores causes cells to synthesize a collagen matrix which is aligned with the pore walls. This behaviour could be used to control or guide the desired bone structure within biodegradable structures. Cells aligned within lamellar shaped pores tend to form cortical bone, while a trabecular bone structure could be achieved by designing a structure with big spherical shaped pores.

Cell proliferation depends on the available surface area for cells to multiply and may also be dependent on the surface roughness. However, due to disparity in the results no decisive conclusion could be drawn regarding the effects of surface roughness on cell proliferation.

Porous biomaterials with a pore size larger than 400 µm seem to be beneficial for angiogenesis. Blood vessels provide the cells and nutrients needed for bone formation and grow into the porous biomaterial through the interconnected pore network. When the void space is clearly defined, blood vessels will grow in a controlled way, while a random inner architecture leads to an uncontrolled network of blood vessels. It is clear that a well vascularized structure is important for the formation of new bone.

The addition of HA or CaP increases the surface roughness and chemistry, thereby improving cell adhesion and promoting a well-spread morphology. A well-spread morphology is associated with osteogenic differentiation as shown in a study by McBeath *et al.*,<sup>53</sup> and seems to be the case in more studies. However, it was seen that in some studies a less spread morphology could also induce osteogenic differentiation. Cell differentiation into osteoblasts is also promoted by structures with an elastic modulus close to that of bone.

More new bone is found in structures with bigger pores, a higher porosity, the addition of chitosan or HA, a higher surface roughness, and a stiffness close to the elastic modulus of bone. A higher surface roughness promotes mechanical interlocking, which improves the bond strength between the porous biomaterial and the host bone.

These findings show that different cell responses are connected to each other. Although the seeding efficiency is well studied in different papers, a higher seeding efficiency is not crucial for consequent cell responses. Even though a higher seeding efficiency was found in porous biomaterials with smaller pores, small pores do not seem to be beneficial for other steps in the bone regeneration process. Good perfusion of oxygen and nutrients is preferable for high cell viability and proliferation, and osteogenic differentiation and blood vessel formation are important for the mineralization of the synthesized collagen matrix and bone formation.





Future research should focus on optimizing the diffusion of oxygen and nutrients to the inner regions of a bone substitute to promote osteogenic differentiation and the formation of blood vessels.

This paper shows that different aspects have to be considered when designing a porous biomaterial for bone regeneration. With the information available, it is impossible to say what value should be chosen for every architectural parameter to design the 'ideal' porous biomaterial. Depending on the biomaterial of the bone substitute, an appropriate porosity, pore size, and pore shape should be chosen to make the porous biomaterial suitable for the implantation site. By designing a tortuous void network, the cell suspension is more guided through the scaffold which increases the available surface and time for the cells to attach to the surface of the porous biomaterial. It is more or less clear that a pore size smaller than 100  $\mu\text{m}$  should be avoided, that pores smaller than 200–300  $\mu\text{m}$  may limit cell migration and proliferation and that pores larger than 400  $\mu\text{m}$  are preferable for angiogenesis.

## References

- Y. Reinwald, R. Johal, A. Ghaemmaghami, F. Rose, S. Howdle and K. Shakesheff, *Polymer*, 2014, **55**, 435–444.
- D. Nadeem, C.-A. Smith, M. J. Dalby, R. D. Meek, S. Lin, G. Li and B. Su, *Biofabrication*, 2015, **7**, 015005.
- C. E. Holy, M. S. Shoichet and J. E. Davies, *J. Biomed. Mater. Res.*, 2000, **51**, 376–382.
- B. Seo, W. Sonoyama, T. Yamaza, C. Coppe, T. Kikuri, K. Akiyama, J. Lee and S. Shi, *Oral Dis.*, 2008, **14**, 428–434.
- J. Park, J. Ries, K. Gelse, F. Kloss, K. Von Der Mark, J. Wiltfang, F. Neukam and H. Schneider, *Gene Ther.*, 2003, **10**, 1089–1098.
- Z. S. Patel, S. Young, Y. Tabata, J. A. Jansen, M. E. Wong and A. G. Mikos, *Bone*, 2008, **43**, 931–940.
- M. P. Lutolf, F. E. Weber, H. G. Schmoekel, J. C. Schense, T. Kohler, R. Müller and J. A. Hubbell, *Nat. Biotechnol.*, 2003, **21**, 513–518.
- H. H. Lu, S. F. El-Amin, K. D. Scott and C. T. Laurencin, *J. Biomed. Mater. Res., Part A*, 2003, **64**, 465–474.
- D. F. Williams, *Biomaterials*, 2008, **29**, 2941–2953.
- P. H. Warnke, T. Douglas, P. Wollny, E. Sherry, M. Steiner, S. Galonska, S. T. Becker, I. N. Springer, J. Wiltfang and S. Sivananthan, *Tissue Eng., Part C*, 2008, **15**, 115–124.
- J. Van der Stok, O. P. Van der Jagt, S. Amin Yavari, M. F. De Haas, J. H. Waarsing, H. Jahr, E. M. Van Lieshout, P. Patka, J. A. Verhaar and A. A. Zadpoor, *J. Orthop. Res.*, 2013, **31**, 792–799.
- S. Van Bael, Y. C. Chai, S. Truscetto, M. Moesen, G. Kerckhofs, H. Van Oosterwyck, J.-P. Kruth and J. Schrooten, *Acta Biomater.*, 2012, **8**, 2824–2834.
- S. A. Yavari, S. Ahmadi, R. Wauthle, B. Pouran, J. Schrooten, H. Weinans and A. Zadpoor, *J. Mech. Behav. Biomed. Mater.*, 2015, **43**, 91–100.
- J. Wieding, T. Lindner, P. Bergschmidt and R. Bader, *Biomaterials*, 2015, **46**, 35–47.
- J. Wieding, A. Jonitz and R. Bader, *Materials*, 2012, **5**, 1336–1347.
- S. A. Yavari, J. van der Stok, Y. C. Chai, R. Wauthle, Z. T. Birgani, P. Habibovic, M. Mulier, J. Schrooten, H. Weinans and A. A. Zadpoor, *Biomaterials*, 2014, **35**, 6172–6181.
- E. García-Gareta, J. Hua and G. W. Blunn, *Journal of J. Biomed. Mater. Res., Part A*, 2015, **103**, 1067–1076.
- X. Fan, B. Feng, Z. Liu, J. Tan, W. Zhi, X. Lu, J. Wang and J. Weng, *J. Biomed. Mater. Res., Part A*, 2012, **100**, 3422–3427.
- X. Liu, S. Wu, K. W. Yeung, Y. Chan, T. Hu, Z. Xu, X. Liu, J. C. Chung, K. M. Cheung and P. K. Chu, *Biomaterials*, 2011, **32**, 330–338.
- A. R. Amini, D. J. Adams, C. T. Laurencin and S. P. Nukavarapu, *Tissue Eng., Part A*, 2012, **18**, 1376–1388.
- K. Kim, D. Dean, J. Wallace, R. Breithaupt, A. G. Mikos and J. P. Fisher, *Biomaterials*, 2011, **32**, 3750–3763.
- C. Correia, S. Bhumiratana, L.-P. Yan, A. L. Oliveira, J. M. Gimble, D. Rockwood, D. L. Kaplan, R. A. Sousa, R. L. Reis and G. Vunjak-Novakovic, *Acta Biomater.*, 2012, **8**, 2483–2492.
- S. Hofmann, H. Hagenmüller, A. M. Koch, R. Müller, G. Vunjak-Novakovic, D. L. Kaplan, H. P. Merkle and L. Meinel, *Biomaterials*, 2007, **28**, 1152–1162.
- M. Stoppato, E. Carletti, V. Sidarovich, A. Quattrone, R. E. Unger, C. J. Kirkpatrick, C. Migliaresi and A. Motta, *J. Bioact. Compat. Polym.*, 2013, **28**, 16–32.
- H.-Y. Mi, X. Jing, M. R. Salick, T. M. Cordie, X.-F. Peng and L.-S. Turng, *J. Mater. Sci.*, 2014, **49**, 2324–2337.
- L. G. Sicchieri, G. E. Crippa, P. T. de Oliveira, M. M. Beloti and A. L. Rosa, *J. Tissue Eng. Regener. Med.*, 2012, **6**, 155–162.
- B. Feng, Z. Jinkang, W. Zhen, L. Jianxi, C. Jiang, L. Jian, M. Guolin and D. Xin, *Biomed. Mater.*, 2011, **6**, 015007.
- J. Qian, M. Xu, A. Suo, T. Yang and X. Yong, *Mater. Lett.*, 2013, **93**, 72–76.
- S. Bhumiratana, W. L. Grayson, A. Castaneda, D. N. Rockwood, E. S. Gil, D. L. Kaplan and G. Vunjak-Novakovic, *Biomaterials*, 2011, **32**, 2812–2820.
- R. J. Kane, H. E. Weiss-Bilka, M. J. Meagher, Y. Liu, J. A. Gargac, G. L. Niebur, D. R. Wagner and R. K. Roeder, *Acta Biomater.*, 2015, **17**, 16–25.
- C. M. Murphy, M. G. Haugh and F. J. O'Brien, *Biomaterials*, 2010, **31**, 461–466.
- P. Yilgor, G. Yilmaz, M. Onal, I. Solmaz, S. Gundogdu, S. Keskil, R. Sousa, R. Reis, N. Hasirci and V. Hasirci, *J. Tissue Eng. Regener. Med.*, 2013, **7**, 687–696.
- C. Wu, Y. Luo, G. Cuniberti, Y. Xiao and M. Gelinsky, *Acta Biomater.*, 2011, **7**, 2644–2650.
- P. Yilgor, R. A. Sousa, R. L. Reis, N. Hasirci and V. Hasirci, *J. Mater. Sci.: Mater. Med.*, 2010, **21**, 2999–3008.
- G. Kumar, M. S. Waters, T. M. Farooque, M. F. Young and C. G. Simon, *Biomaterials*, 2012, **33**, 4022–4030.
- J. R. Woodard, A. J. Hilldore, S. K. Lan, C. Park, A. W. Morgan, J. A. C. Eurell, S. G. Clark, M. B. Wheeler,



- R. D. Jamison and A. J. W. Johnson, *Biomaterials*, 2007, **28**, 45–54.
- 37 L. Lao, Y. Wang, Y. Zhu, Y. Zhang and C. Gao, *J. Mater. Sci.: Mater. Med.*, 2011, **22**, 1873–1884.
- 38 A. Salerno, D. Guarnieri, M. Iannone, S. Zeppetelli and P. A. Netti, *Tissue Eng., Part A*, 2010, **16**, 2661–2673.
- 39 J. Sanz-Herrera, J. Garcia-Aznar and M. Doblare, *Biomech. Model. Mechanobiol.*, 2008, **7**, 355–366.
- 40 C. Jungreuthmayer, S. W. Donahue, M. J. Jaasma, A. A. Al-Munajjed, J. Zanghellini, D. J. Kelly and F. J. O'Brien, *Tissue Eng., Part A*, 2008, **15**, 1141–1149.
- 41 A. A. Zadpoor, *Biomater. Sci.*, 2015, **3**, 231–245.
- 42 M. Bohner, Y. Loosli, G. Baroud and D. Lacroix, *Acta Biomater.*, 2011, **7**, 478–484.
- 43 M. Dias, P. Fernandes, J. Guedes and S. Hollister, *J. Biomech.*, 2012, **45**, 938–944.
- 44 I. Marcos-Campos, D. Marolt, P. Petridis, S. Bhumiratana, D. Schmidt and G. Vunjak-Novakovic, *Biomaterials*, 2012, **33**, 8329–8342.
- 45 H.-I. Chang and Y. Wang, in *Regenerative Medicine and Tissue Engineering – Cells and Biomaterials*, ed. P. D. Eberli, InTech, 2011, ch. 27, pp. 569–588.
- 46 B. B. Mandal, A. Grinberg, E. S. Gil, B. Panilaitis and D. L. Kaplan, *Proc. Natl. Acad. Sci. U. S. A.*, 2012, **109**, 7699–7704.
- 47 D. Wendt, A. Marsano, M. Jakob, M. Heberer and I. Martin, *Biotechnol. Bioeng.*, 2003, **84**, 205–214.
- 48 P. Codogno and A. J. Meijer, *Cell Death Differ.*, 2005, **12**, 1509–1518.
- 49 S. S. Kim, H. Utsunomiya, J. A. Koski, B. M. Wu, M. J. Cima, J. Sohn, K. Mukai, L. G. Griffith and J. P. Vacanti, *Ann. Surg.*, 1998, **228**, 8.
- 50 N. Q. Balaban, U. S. Schwarz, D. Riveline, P. Goichberg, G. Tzur, I. Sabanay, D. Mahalu, S. Safran, A. Bershadsky and L. Addadi, *Nat. Cell Biol.*, 2001, **3**, 466–472.
- 51 M. L. Gardel, I. C. Schneider, Y. Aratyn-Schaus and C. M. Waterman, *Annu. Rev. Cell Dev. Biol.*, 2010, **26**, 315.
- 52 C. S. Chen, J. L. Alonso, E. Ostuni, G. M. Whitesides and D. E. Ingber, *Biochem. Biophys. Res. Commun.*, 2003, **307**, 355–361.
- 53 R. McBeath, D. M. Pirone, C. M. Nelson, K. Bhadriraju and C. S. Chen, *Dev. Cell*, 2004, **6**, 483–495.
- 54 K. Anselme, *Biomaterials*, 2000, **21**, 667–681.
- 55 F. M. Watt and W. T. Huck, *Nat. Rev. Mol. Cell Biol.*, 2013, **14**, 467–473.
- 56 H. Tal, *Introductory Chapter, Bone Regeneration*, InTech, 2012.
- 57 E. Birmingham, G. Niebur and P. McHugh, *Eur. Cells Mater.*, 2012, **23**, 13–27.
- 58 A. M. Martins, C. M. Alves, R. L. Reis, A. G. Mikos and F. K. Kasper, *Biological Interactions on Materials Surfaces*, Springer, 2009, pp. 263–281.
- 59 O. Matsubara, E. Hase, T. Minamikawa, T. Yasui and K. Sato, *SPIE BiOS. International Society for Optics and Photonics*, 2016, 971222.
- 60 Q. L. Loh and C. Choong, *Tissue Eng., Part B*, 2013, **19**, 485–502.
- 61 W. Murphy, C. Simmons, D. Kaigler and D. Mooney, *J. Dent. Res.*, 2004, **83**, 204–210.
- 62 H. Wang, W. Zhi, X. Lu, X. Li, K. Duan, R. Duan, Y. Mu and J. Weng, *Acta Biomater.*, 2013, **9**, 8413–8421.
- 63 X. Li, Y. Huang, L. Zheng, H. Liu, X. Niu, J. Huang, F. Zhao and Y. Fan, *J. Biomed. Mater. Res., Part A*, 2014, **102**, 1092–1101.
- 64 X. Yu, Z. Xia, L. Wang, F. Peng, X. Jiang, J. Huang, D. Rowe and M. Wei, *J. Mater. Chem.*, 2012, **22**, 9721–9730.
- 65 M. Witkowska-Zimny, K. Walenko, E. Wrobel, P. Mrowka, A. Mikulska and J. Przybylski, *Cell Biol. Int.*, 2013, **37**, 608–616.
- 66 J. A. Helsen and Y. Missirlis, *Biomaterials*, Springer, 2010, pp. 269–289.
- 67 T. Van Cleynenbreugel, J. Schrooten, H. Van Oosterwyck and J. Vander Sloten, *Med. Biol. Eng. Comput.*, 2006, **44**, 517–525.
- 68 B. V. Krishna, S. Bose and A. Bandyopadhyay, *Acta Biomater.*, 2007, **3**, 997–1006.
- 69 W. Xue, B. V. Krishna, A. Bandyopadhyay and S. Bose, *Acta Biomater.*, 2007, **3**, 1007–1018.
- 70 A. Bandyopadhyay, F. Espana, V. K. Balla, S. Bose, Y. Ohgami and N. M. Davies, *Acta Biomater.*, 2010, **6**, 1640–1648.
- 71 N. G. Mehr, X. Li, M. B. Ariganello, C. D. Hoemann and B. D. Favis, *J. Mater. Sci.: Mater. Med.*, 2014, **25**, 2083–2093.
- 72 Y. Zhang, W. Fan, Z. Ma, C. Wu, W. Fang, G. Liu and Y. Xiao, *Acta Biomater.*, 2010, **6**, 3021–3028.
- 73 P. Y. Huri, B. A. Ozilgen, D. L. Hutton and W. L. Grayson, *Biomed. Mater.*, 2014, **9**, 045003.
- 74 C. Wu, Y. Zhang, Y. Zhu, T. Friis and Y. Xiao, *Biomaterials*, 2010, **31**, 3429–3438.
- 75 P. K. Mattila and P. Lappalainen, *Nat. Rev. Mol. Cell Biol.*, 2008, **9**, 446–454.
- 76 C. Jungreuthmayer, M. J. Jaasma, A. A. Al-Munajjed, J. Zanghellini, D. J. Kelly and F. J. O'Brien, *Med. Eng. Phys.*, 2009, **31**, 420–427.
- 77 K. Matsuo and N. Irie, *Arch. Biochem. Biophys.*, 2008, **473**, 201–209.
- 78 F. Lecanda, D. A. Towler, K. Ziambaras, S.-L. Cheng, M. Koval, T. H. Steinberg and R. Civitelli, *Mol. Biol. Cell*, 1998, **9**, 2249–2258.
- 79 M. G. Vander Heiden, L. C. Cantley and C. B. Thompson, *Science*, 2009, **324**, 1029–1033.
- 80 R. A. Carano and E. H. Filvaroff, *Drug Discovery Today*, 2003, **8**, 980–989.
- 81 A. Penk, Y. Förster, H. A. Scheidt, A. Nimptsch, M. C. Hacker, M. Schulz-Siegmund, P. Ahnert, J. Schiller, S. Rammelt and D. Huster, *Magn. Reson. Med.*, 2013, **70**, 925–935.
- 82 D. W. Huttmacher, M. Sittlinger and M. V. Risbud, *Trends Biotechnol.*, 2004, **22**, 354–362.
- 83 A. Abarrategi, C. Moreno-Vicente, F. J. Martínez-Vázquez, A. Civantos, V. Ramos, J. V. Sanz-Casado, R. Martínez-Corriá, F. H. Perera, F. Mulero and P. Miranda, *PLoS One*, 2012, **7**, e34117.
- 84 J. Y. Park, D. H. Lee, E. J. Lee and S.-H. Lee, *Lab Chip*, 2009, **9**, 2043–2049.



- 85 S. Scaglione, P. Giannoni, P. Bianchini, M. Sandri, R. Marotta, G. Firpo, U. Valbusa, A. Tampieri, A. Diaspro and P. Bianco, *Sci. Rep.*, 2012, **2**, 274.
- 86 J. Zhao, W. Han, H. Chen, M. Tu, S. Huan, G. Miao, R. Zeng, H. Wu, Z. Cha and C. Zhou, *J. Mater. Sci.: Mater. Med.*, 2012, **23**, 517–525.
- 87 X. Liu, M. N. Rahaman and Q. Fu, *Acta Biomater.*, 2013, **9**, 4889–4898.
- 88 T. Guda, J. A. Walker, B. Singleton, J. Hernandez, D. S. Oh, M. R. Appleford, J. L. Ong and J. C. Wenke, *J. Biomater. Appl.*, 2014, **28**, 1016–1027.
- 89 F. Guilak, D. M. Cohen, B. T. Estes, J. M. Gimble, W. Liedtke and C. S. Chen, *Cell Stem Cell*, 2009, **5**, 17–26.
- 90 D. A. Puleo and R. Bizios, *Biological interactions on materials surfaces: understanding and controlling protein, cell, and tissue responses*, Springer Science & Business Media, 2009.
- 91 D. D. Deligianni, N. Katsala, S. Ladas, D. Sotiropoulou, J. Amedee and Y. Missirlis, *Biomaterials*, 2001, **22**, 1241–1251.
- 92 D. D. Deligianni, N. D. Katsala, P. G. Koutsoukos and Y. F. Missirlis, *Biomaterials*, 2000, **22**, 87–96.
- 93 R. A. Gittens, T. McLachlan, R. Olivares-Navarrete, Y. Cai, S. Berner, R. Tannenbaum, Z. Schwartz, K. H. Sandhage and B. D. Boyan, *Biomaterials*, 2011, **32**, 3395–3403.
- 94 E. A. Nauman, K. Fong and T. Keaveny, *Ann. Biomed. Eng.*, 1999, **27**, 517–524.
- 95 R. Bosco, J. Van Den Beucken, S. Leeuwenburgh and J. Jansen, *Coatings*, 2012, **2**, 95–119.
- 96 M. Navarro, A. Michiardi, O. Castano and J. Planell, *J. R. Soc., Interface*, 2008, **5**, 1137–1158.
- 97 M. F. Ashby and D. Cebon, *J. Phys. IV*, 1993, **3**, C7-1–C7-9.
- 98 D. E. Discher, P. Janmey and Y.-L. Wang, *Science*, 2005, **310**, 1139–1143.
- 99 A. S. Mao, J.-W. Shin and D. J. Mooney, *Biomaterials*, 2016, **98**, 184–191.
- 100 S. Tan, J. Y. Fang, Z. Yang, M. E. Nimni and B. Han, *Biomaterials*, 2014, **35**, 5294–5306.
- 101 J. Lee, A. A. Abdeen, T. H. Huang and K. A. Kilian, *J. Mech. Behav. Biomed. Mater.*, 2014, **38**, 209–218.
- 102 J.-P. Kruth, P. Mercelis, J. Van Vaerenbergh, L. Froyen and M. Rombouts, *Rapid prototyping journal*, 2005, **11**, 26–36.
- 103 J. M. Sobral, S. G. Caridade, R. A. Sousa, J. F. Mano and R. L. Reis, *Acta Biomater.*, 2011, **7**, 1009–1018.
- 104 F. Bobbert, K. Lietaert, A. Eftekhari, B. Pouran, S. Ahmadi, H. Weinans and A. Zadpoor, *Acta Biomater.*, 2017, **53**, 572–584.

